CrossMark

ORIGINAL RESEARCH

A combination of experimental and finite element analyses of needle–tissue interaction to compute the stresses and deformations during injection at different angles

Mahdi Halabian[1,2] · Borhan Beigzadeh[1] · Alireza Karimi[1,2,3] ·
Hadi Asgharzadeh Shirazi[1,2] · Mohammad Hasan Shaali[1]

Abstract One of the main clinical applications of the needles is its practical usage in the femoral vein catheterization. Annually more than two million peoples in the United States are exposed to femoral vein catheterization. How to use the input needles into the femoral vein has a key role in the sense of pain in post-injection and possible injuries, such as tissue damage and bleeding. It has been shown that there might be a correlation between the stresses and deformations due to femoral injection to the tissue and the sense of pain and, consequently, injuries caused by needles. In this study, the stresses and deformations induced by the needle to the femoral tissue were experimentally and numerically investigated in response to an input needle at four different angles, i.e., 30°, 45°, 60°, and 90°, via finite element method. In addition, a set of experimental injections at different angles were carried out to compare the numerical results with that of the experimental ones, namely pain score. The results revealed that by increasing the angle of injection up to 60°, the strain at the interaction site of the needle–tissue is increased accordingly while a significant falling is observed at the angle of 90°. In contrast, the stress due to injection was decreased at the region of needle–tissue interaction with showing the lowest one at the angle of 90°. Experimental results were also well confirmed the numerical observations since the lowest pain score was seen at the angle of 90°. The results suggest that the most effective angle of injection would be 90° due to a lower amount of stresses and deformations compared to the other angles of injection. These findings may have implications not only for understating the stresses and deformations induced during injection around the needle–tissue interaction, but also to give an outlook to the doctors to implement the most suitable angle of injection in order to reduce the pain as well as post injury of the patients.

1 Introduction

Needles, at various geometries and shapes, have wide range of applications in many clinical areas as well as medical diagnostic procedures, including biopsy to obtain a tissue sample for testing, anesthesia drug injections, and brachytherapy radioactive seed implants for cancer treatment [1]. It has been reported that annually there are more than 12 billion injections across the world [2]. Due to the extensive practical application of needles in the medical injections without numbing drugs, such as muscular injection, fear of injection as well as pain remain as an unsolved problem yet. Forty percent of patients in a particular study have declared that intramuscular injection is one of the most painful injections which is accompanied by pain and perhaps subsequent injury. In addition, it has been estimated that around 5.3 and 22 % of peoples have extreme or average level of fear from injection, respectively [3]. Several factors play critical roles in the pain at

✉ Alireza Karimi
karimia@outlook.com

1 School of Mechanical Engineering, Iran University of Science and Technology, Tehran 16846, Iran

2 Tissue Engineering and Biological Systems Research Laboratory, School of Mechanical Engineering, Iran University of Science and Technology, Tehran 16886, Iran

3 Department of Mechanical Engineering, Kyushu University, 744 Motooka, Nishi-ku, Fukuoka 819-0395, Japan

the injection site, such as size and shape of the needles, depth, and the specific location of injection as well as the rate and speed of injection, which should be investigated with the standard methods in the field. Many efforts have been devoted to propose a way to minimize the pain and side effects of injection, including distraction and topical cold therapy, administration of oral glucose, changing of the pressure, applying mother hug, improving the location of injection, and finally needle tip size [4]. Employing of input needle in femoral vein catheterization is another major application of needles. Each year more than 2 million peoples in the United States are subjected to the femoral vein catheterization. The first step in this procedure is the femoral artery access, which is accompanied with the probability of 3–5 %, contains the risk of complications, including bleeding, severed arteries, and thrombosis [5]. It seems that the way how to employ the input needles catheterization has an effective role in a sense of pain after the end of injection and possible injuries, such as tissue damage. Moreover, previous studies revealed that there are some correlations between the stresses and deformations induced in the tissue and the sense of pain and injuries caused by needles.

So far there have been many reports on the impacts of geometry and material properties of the needles, and tissue behavior on the needle–tissue interaction. Finocchietti et al. [6] showed that the evoked muscle pain by pressure stimulation of the tissues is mainly related to the surface muscle strain. They also benefitted from finite element (FE) simulation to indicate that the level of pain that would induce due to injection could be different based on the softness and stiffness of the muscles [7]. Some other studies focused on the forces in the needle shaft and consequently tissue behavior via a set of tissue measurement system and soft tissue deformation models [8]. Alja'afreh [9] provided an energy-based fracture mechanics approach to exhibit that, increasing the velocity of needle can reduce the tissue motion during the insertion process. Keehan and Gergely [10] performed an experimental study to evaluate the role of needle material in the pain of injections. They benefitted from a CoCr alloy, 17-7 PH, and nano-flex stainless steels (SSs) materials to recommend them as an alternative to be used instead of conventional SS 304 material for hypotube and needle materials. In this field, Xu et al. [11] also

proposed a shape memory alloy (SMA) as an inner needle material which enables to diminish the pain of injection. The deflection of brachytherapy needles with different tip geometries was also investigated [12]. The results revealed that the continuous rotation of needle can significantly reduce not only the deflection but also the pain of injection. Mahvash and Dupont [13] analyzed the possibility of rupture that can occur during needle insertion inside the multilayered biological materials. They developed a qualitative fracture model that relates rupture force to the contact area as well as the material properties of the tissue. An experimental tactile force simulator was proposed for
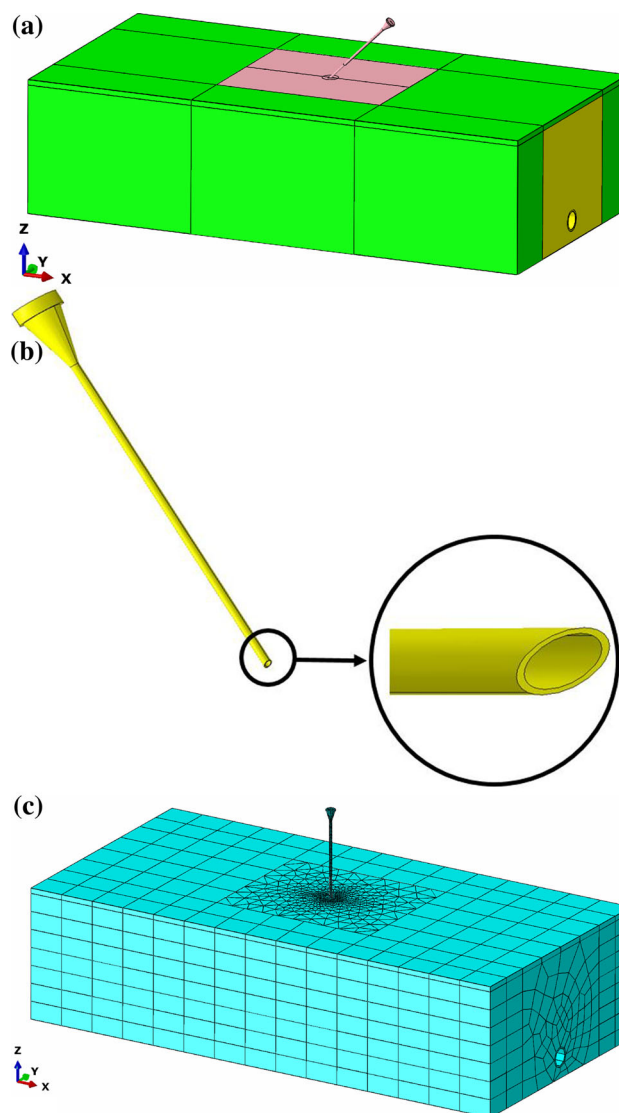

Fig. 1 The finite element (FE) model of the femur tissue and needle in a rectangular cube configuration, including **a** the needle–tissue interaction, **b** the needle itself, and **c** the meshed needle–tissue interaction. The contact region, which needle is in contact with tissue, was more intensively meshed for further accurate numerical simulation

Table 1 The insertion parameters of the needle for injection

Injection angle (deg)	Traveled distance
90	a_s
60	$1.15a_s$
45	$1.91a_s$
30	$2a_s$

uniaxial needle action in which the force resisting progress of the needle is derived from measured data [14]. Reed et al. [15] developed a fundamental model of a long thin object rotating inside a continuous medium. They illustrated the practical significance of torque generated by the needle–tissue interface and formulated a model of the rotational dynamics that can be implemented into path planners and position controllers for steerable needles. Okamura et al. [16] presented a methodology for the measurement of stiffness, friction, cutting forces, and needle geometry effects during the insertion of needles into soft tissues. Recently, the effects of insertion and withdrawal forces induced by needles with standard traumatic bevel were comprehensively compared to those with a novel asymmetrical bevel in vitro [17]. They proposed a novel design which needs less force compared to the standard version to penetrate a soft thin membrane.

Boonma et al. [18] presented a nonlinear analytical model to quantify the forces due to micro needle insertion at different micro needle geometries. Very recently, a sophisticated approach was proposed to model the features of translational friction during needle–tissue interaction [19]. Their results suggest that the mappings of static friction are inadequate for describing the existence of transient nature. Matthews et al. [20] used indentation and needle insertion to investigate the biomechanical stresses and deformations in the human eye. The preliminary experimental findings from a novel four-needle coaxial electro-hydro-dynamic (EHD) device demonstrated that the four-layered structures in both particle and fiber form can be obtained [21]. There were also some studies benefitted from the FE analysis to investigate the role of various tip angles in biodegradable polymers [22] and to simulate the dynamic [23] and cohesive [24] behaviors of needle
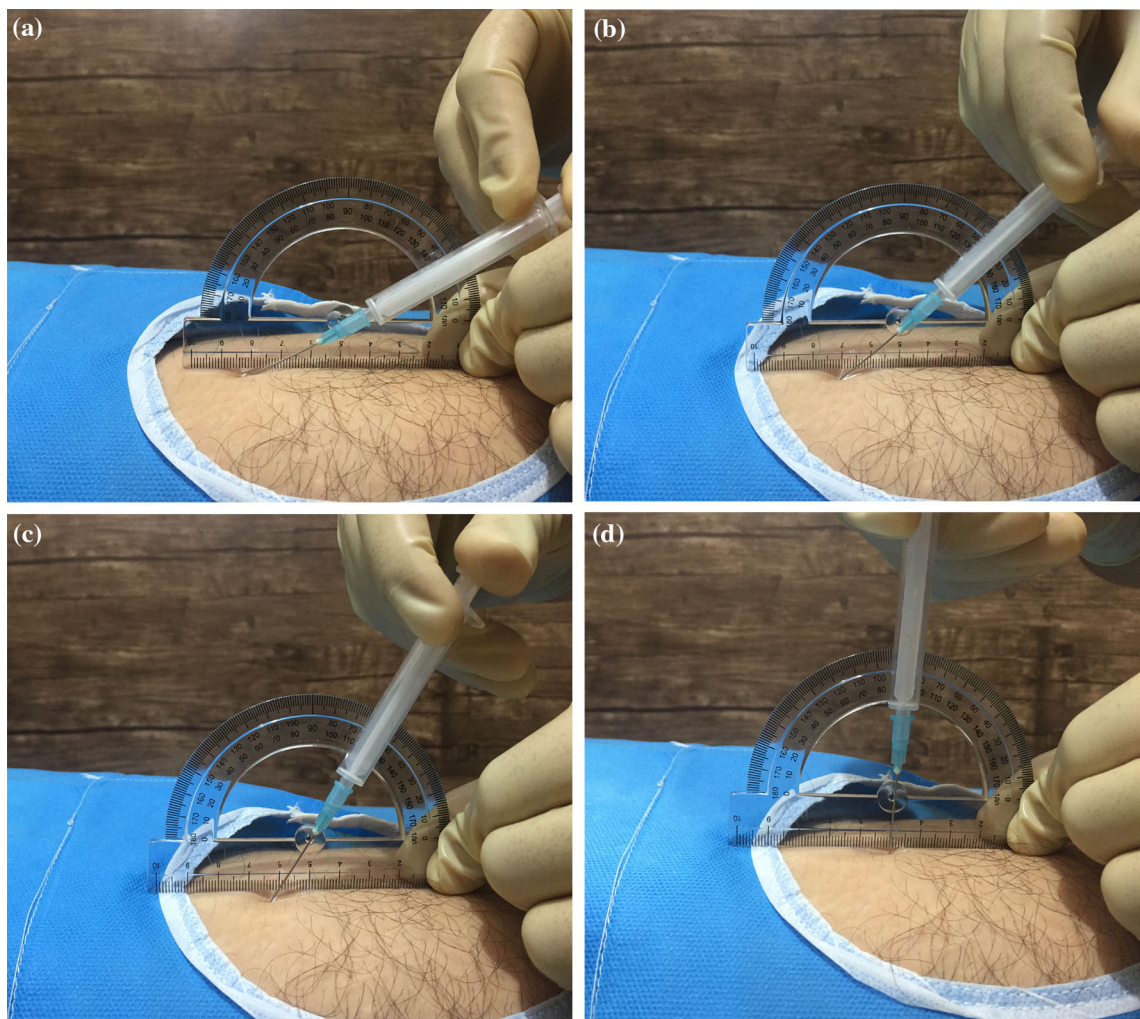

Fig. 2 Experimental study was carried out to confirm the numerical results. To do this, a specific drug has been injected at a particular angle to 49 individuals in a hospital. A typical configuration of the injection process at different angles, including **a** 30, **b** 45, **c** 60, and **d** 90

Table 2 The mechanical properties of the different soft tissues in the model

Tissue type	Young's modulus (MPa)	Poisson's ratio
Skin	2.10	0.30
Soft tissue	0.11	0.30
Vessel	1.23	0.25
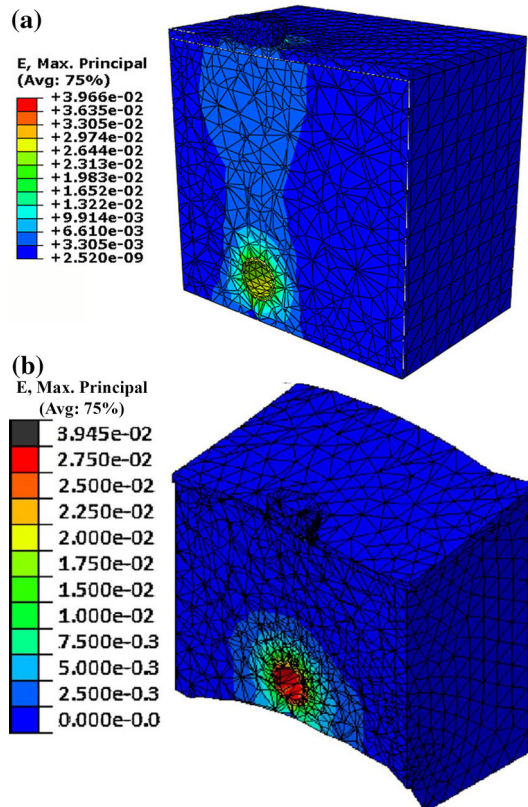
Fig. 3 The agreement of the **a** our numerical simulation with that of **b** Miller et al. [5] has been assessed through the strain distribution in a cube femur under the same simulation conditions

insertion into the soft tissue using arbitrary Lagrangian–Eulerian based FE models. These studies mainly perform an experimental study and thereafter confirm their experimental observations with that of the FE ones.

However, so far there is a lack of knowledge as to which angle of injection would provide a less pain as well as post-injury to the soft tissue. Therefore, in this study the stresses and deformations in the femoral vein tissue were investigated in response to input needle catheterization at the angles of 30°, 45°, 60°, and 90° using experimental approach and FE analysis. It was the authors expectation to reveal the correlation of injection angle and pain, and finally to recommend a specific angle for a low pain injection.

2 Materials and methods

2.1 Model properties

The configuration, geometry, and the mechanical properties of the established femoral vein model were adopted from the previously published data [5]. The model was consisted of a rectangular cube of a femur tissue set which is formed from slices of skin, soft tissues (including fat, muscle, and ligament), and the femoral artery. The femoral vein tissue was considered as rectangular cube to strength the accuracy of the FE simulation and prevent error possibility [5]. The rectangular configuration of the model not only would provide a suitable modeling condition but also enables us to define a better boundary condition for the FE model. The insertion parameters of the model are summarized in Table 1. The mechanical behavior of the soft tissues in the current model was considered to be elastic and incompressible. The geometry of the different parts were constructed in CATIA V5R21 (Dassault Systèmes Americas Corp, MA, United States) and then the parts were transferred to ABAQUS V6.10 (Dassault Systèmes Americas Corp, MA, United States) in order to perform numerical analyses. The geometry of the rectangular cube of the femur tissue and needle is displayed in Fig. 1. The needle includes the bevel tip type with an angle of 45° based on the geometry of I.V. Catheter (Catheter O. D. 1.10 mm, Demophorius Healthcare®, Cyprus). In this study, in order to find the most suitable angle of injection, four different angles have been chosen, including 30°, 45°, 60°, and 90° respect to the skin surface.

2.2 Loading and boundary conditions

At first, the needle was directed with a speed rate of 8 mm/s into the tissue to fulfil the initial preconditioning for the tissue [8]. The needle was only allowed to move in the direction that needle angle is made to the skin. Since the mechanical property of the needle is much harder than that of the soft tissues, the needle was considered to behave like a rigid material. The pressure of the blood flow was assumed to remain uniformly with a constant value of 0.01 MPa [5]. The bottom of the tissue was fully constrained in all directions and all edges of the vessel were fixed in the both sides of the tissue. The fixed boundary conditions were chosen to be a bit far from the region of needle–tissue interaction to provide the most effective condition with least influence on the external surfaces. In the modeling, two distinct geometries were combined, including one for the central part (the area of needle penetration) and one for the peripheral part. The interface of these two parts were defined to be "tie" and thereafter

these parts were meshed with "hexagonal" and "sweep" elements, respectively. In addition, since needle tip is very sharp, the region of needle–tissue interaction was set to be node released to avoid stress singularity. Furthermore, a more dense mesh was distributed in the needle–tissue contact region to fulfil a more precise simulation outcomes.

2.3 Experimental validation

A group of 49 patients were selected to be injected at each needle angle, including 30°, 45°, 60°, and 90° (Department of cardiovascular surgery, Day hospital, Tehran, Iran). Since the patients were required to be injected weekly, there were suitable access to all of them in 4 weeks. The position and angle of injections are presented in Fig. 2. A questionary form was provided and the patients were asked to express their sense of pain as a score from 0 to 20, as 0 stands for the lowest and 20 stands for the highest level of pain. The scores were then interpreted as the pain score and recorded weekly for each individual for 4 weeks in a way that in the first week all 49 patients were injected at 30° and in the last week (4th week) at 90°. The results were finally reported as mean of the scores ± standard deviation.

2.4 Numerical validation

The convergence of the FE analysis was investigated through a mesh density study in order to obtain a set of reliable data. In the mesh convergence analysis, the modification of mesh volume, stress, and strain distribution were obtained in the simulation model. This simulation is continued until the relative errors become <1 % (it refers to the, for example, value of stress between the two sequences of mesh analysis). The details of the finest mesh volume are listed in Table 2. Moreover, a comparison between the results of the present work and that of the

others has been performed under the same simulation conditions to confirm the numerical observations [5]. Figure 3 illustrates the strain distribution in the cube of femur tissue which confirms its agreement with our results. The mesh under the tip of the needle is illustrated in Fig. 4. Those are small enough that the skin can be easily deformed (Table 3).

3 Results and discussion

Previous studies reported that the sensitivity of nerve receptors which react to injury in the deep tissue is less than that of the superficial layers of the tissue. In the other words, the mechanical sensitivity of these receptors is strongly associated with the strain in tissue [6]. Hence, the threshold of sensitivity in the nerve receptors is sensitive to mechanical alterations and would react and increase the strain in the tissue [6]. Consequently, it is expected that the stress and strain concentration in a segment of the tissue can be interpreted as a feeling of pain or injury. This study was aimed to perform a combination of experimental and numerical analyses to find the most effective angle of injection which brings about less pain and injury. The results revealed that there is a strong correlation between

Table 3 Number of elements and nodes in the simulation model

Injection angle	Number of nodes	Number of elements[a]
System 30°	122,990	90,933
System 45°	123,413	90,372
System 60°	120,792	88,292
System 90°	113,742	82,020

[a] 8 node linear brick, C3D8R and 10 nodes quadratic tetrahedron, C3D10

Fig. 4 The mesh under the tip of the needle
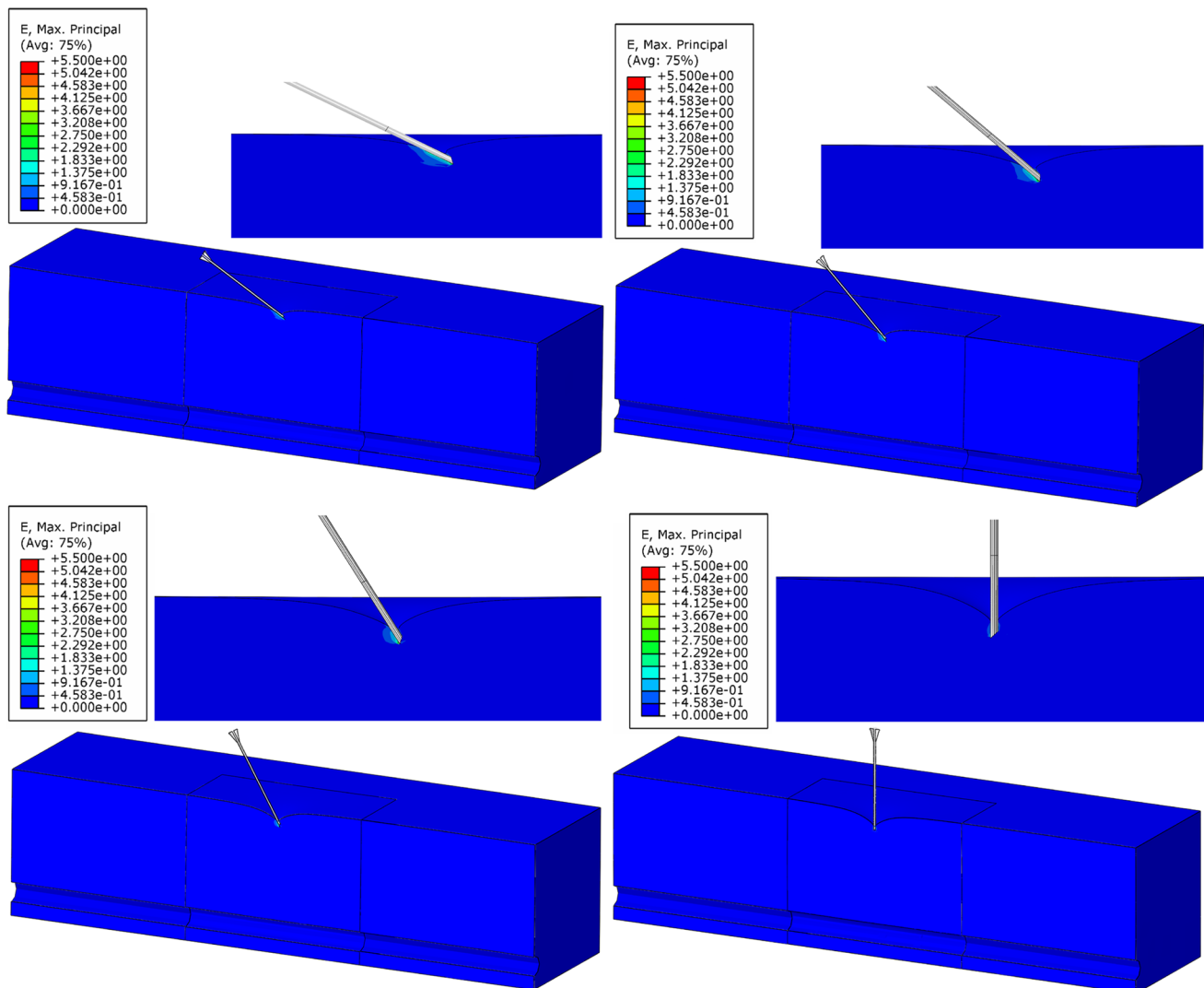

Magnified mesh size
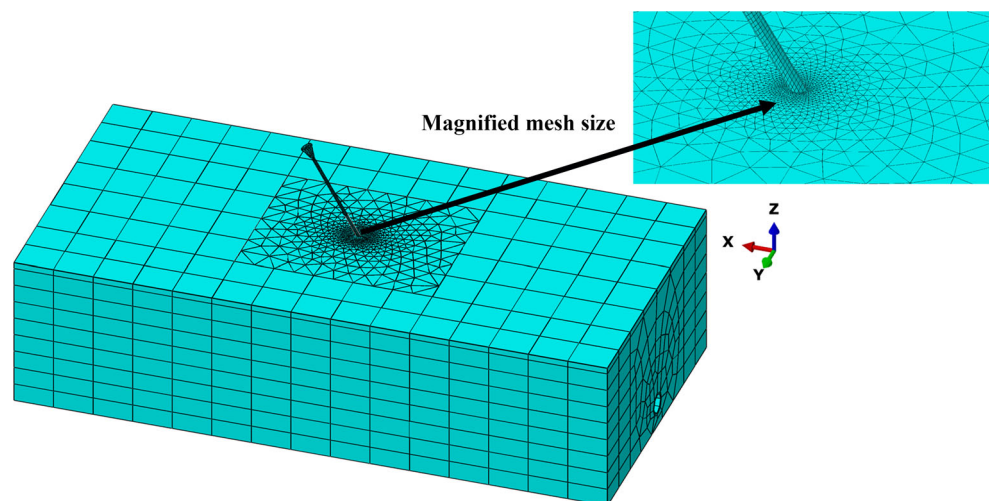
Fig. 5 The distribution of the strain in the region of needle–tissue interaction at different angles, such as **a** 30, **b** 45, **c** 60, and **d** 90

the needle angle and stress/strain distribution around the needle–tissue interaction region. In order to quantify the amount of stress and strain at different needle angles, i.e., 30°, 45°, 60°, and 90°, the FE model of the tissues, including skin, soft tissue, and blood vessels, along with needle were established. It is obvious that due to elastic mechanical behavior assumption for the tissues no rupture is expected to be occurred in the tissues and, as a result, the needle will not penetrate into the deep portions of the tissue. In fact, the main purpose of this study was to evaluate the amount of stresses and deformations right before needle penetrates into the deep segments of the tissue. This is because the distribution of pain receptors in the deeper sections of tissue is lower. The distribution of the strain as the needle applied to the tissue under the angles of 30°, 45°, 60°, and 90° is displayed in Fig. 5. Figure 6 exhibits the stress distribution as the tissue exposed to the needle

insertion with the angles of 30°, 45°, 60°, and 90°. A comparative histogram representation of the maximum strain and stress in the tissues at different angles are illustrated in Fig. 7. When the needle at an angle of 30° respect to the skin surface applied to the tissue, the maximum value of strain is equal to 4.62. This value for angles of 45°, 60° are also equal to 5.19 and 5.49, respectively. Therefore, the values of maximum strain by increasing the angle of injection from the 30° to 60° are increasing accordingly, however, at an angle of 90° there is a sharp falling of strain in the tissue to 1.87 (Fig. 5). The maximum amount of strain is related to the area around the tip of the needle, while the minimum amount of strain is related to the deep parts of tissue which starts to decrease with increasing the needle angle for all the angles. Comparison between these values of stress indicates that the least amount of stress belongs to angle of 90°. In contrast, the
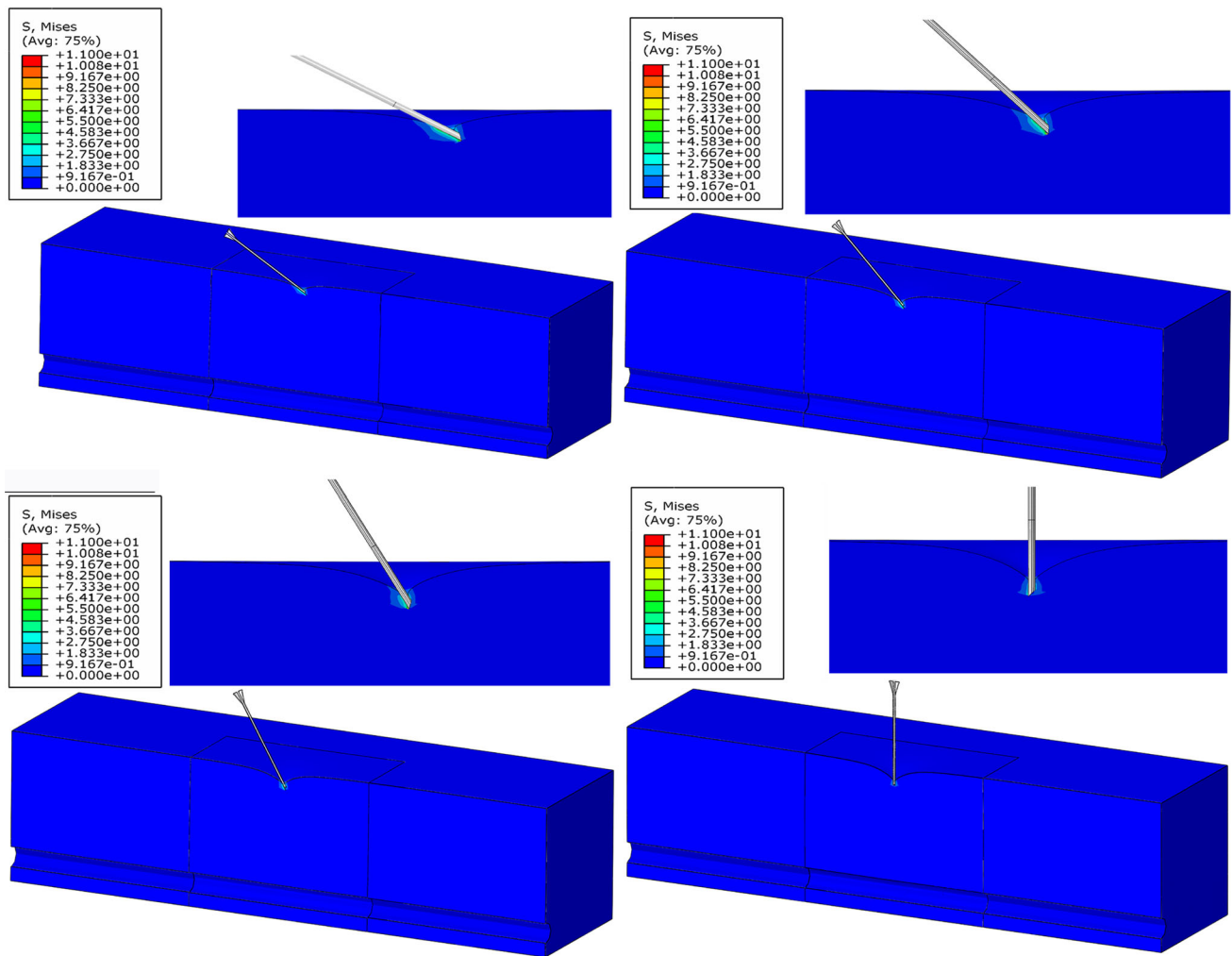
Fig. 6 The distribution of the stress in the region of needle–tissue interaction at different angles, such as **a** 30, **b** 45, **c** 60, and **d** 90

maximum values of stress, which occurs just below the needle, are equal to 10.45 and 9.13 MPa in response to the needle angles of 30° and 60°, respectively. Meanwhile, the max and min amount of stress obtained for the angles of 45° and 90° with values equal to 10.63 and 5.66 MPa, respectively (Fig. 7). This phenomenon can be attributed to the shear stress resulting from needle entrance. In the other words, the magnitudes of shear stress (τ) in the tissue set for the angles of 45° and 90° can be considered to be maximum and minimum (i.e. τ = 0), respectively, for the sake of simplicity. Therefore, since the shear stress is the dominant stress compared to the normal stress in the particular case, the stress caused by the needle with the angle of 90 must be the lowest value of stress in comparison with other cases. Using simple equations governing the issue, it can be found that less stress in the angle of 90° seems to be reasonable and acceptable. For example, the stress is analyzed for the cases of load applied to the elastic sample under the angles of 90° and 45°. As shown in Fig. 8a, when

a perpendicular force is applied to an elastic surface, following equations can be written as:

$$\sigma_{z_{90°}} = \frac{F}{A} \tag{1}$$

$$\sigma' = \frac{1}{\sqrt{2}} \left[(\sigma_x - \sigma_y)^2 + (\sigma_y - \sigma_z)^2 + (\sigma_z - \sigma_x)^2 \right.$$
$$\left. + 6(\tau_{xy}^2 + \tau_{yz}^2 + \tau_{zx}^2) \right]^{1/2} \tag{2}$$

where F is perpendicular force, A is area of elastic surface, $\sigma_{z_{90°}}$ and $\varepsilon_{z_{90°}}$ show stress and strain in z direction for needle in the state of 90°. In addition, σ_x, σ_y, and σ_z display stresses in x, y, and z directions, respectively, as well as τ_{xy}, τ_{yz}, and τ_{zx} are shear stresses. Therefore, by inserting Eq. (1) into (2), we have:

$$\sigma'_{90°} = \sigma_{z_{90°}} \tag{3}$$

where $\sigma'_{90°}$ displays the equivalent von Misses stress under angles of 90°. When force with angle of 45° is applied to an

elastic surface, as shown in Fig. 8b, by decomposing this force into three components following equations can be expressed as:

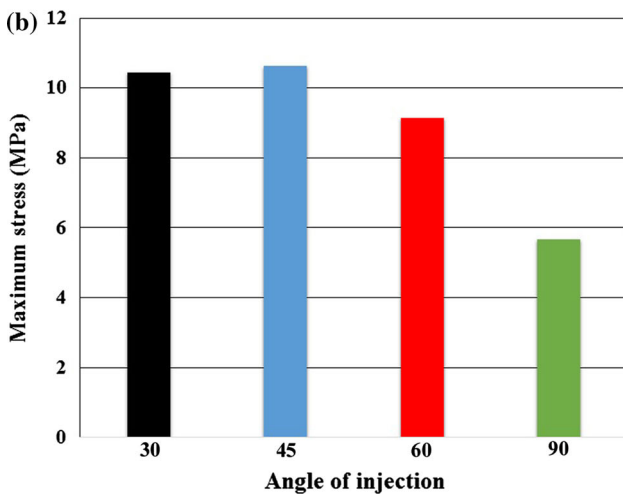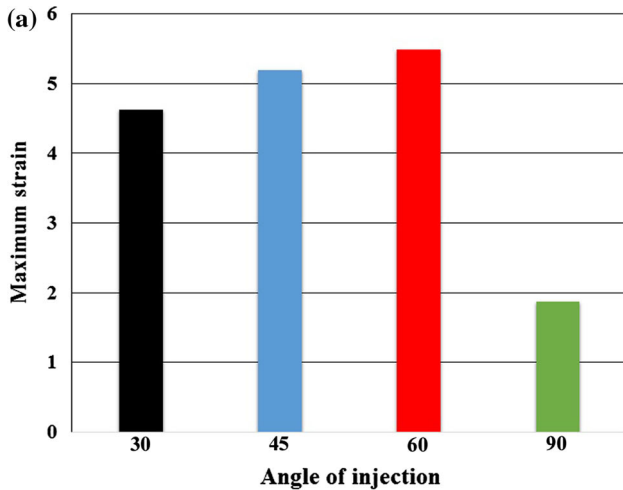$$P = V = \frac{\sqrt{2}}{2} F \tag{4}$$

and

(a)

(b)

Fig. 7 A comparative histogram representation of **a** the maximum strain and **b** the maximum stress on the soft tissue in the contact region of the needle–tissue at different angles, i.e., 30, 45, 60, and 90
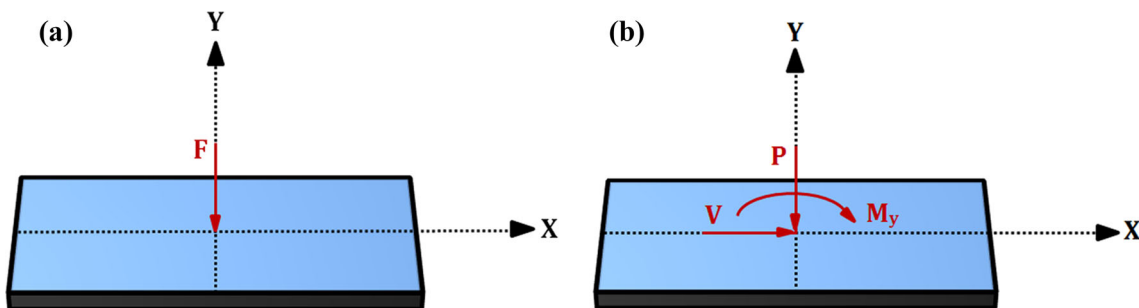
$$\sigma_{z_{45°}} = \frac{P}{A} \pm \frac{M_y c}{I_y}, \quad \begin{cases} M_y = V \cdot z \\ I_y = \frac{1}{12} a \cdot b^3 \end{cases} \tag{5}$$

where F is perpendicular force, and V and P are shear and normal forces, respectively. A is the area of elastic surface, I_y is surface moment of inertia, and $\sigma_{z_{45°}}$ indicates stress in z direction for needle in state of 45°. Z stands the distance of the insertion point that should be implemented into the momentum equation. Moreover, the geometry parameters of a, b, and h are the length, width, and height of the sample, respectively and c displays the distance from the neutral axis. By replacing Eq. (4) into (5) and due to Eq. (1), the flowing equation would be in hand:

$$\sigma_{z_{45°}} = \left[\frac{\sqrt{2}}{2} + 3\sqrt{2} \left(\frac{h}{b^2} \right) z \big|_{z=0}^{z=h} \right] \sigma_{z_{90°}} \tag{6}$$

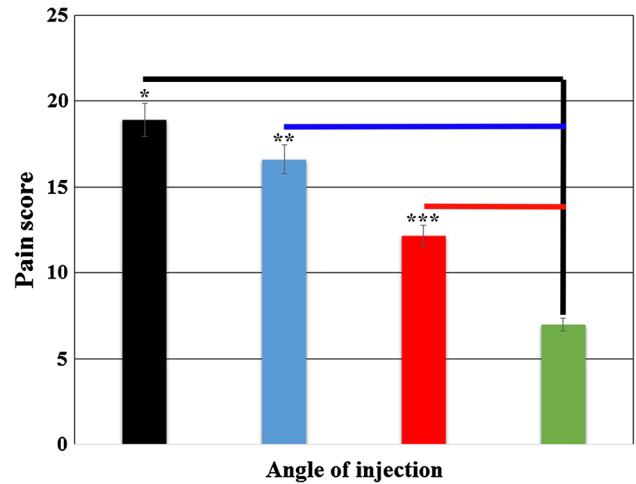with considering Eqs. (1) and (4), we can conclude that:

Fig. 9 In order to quantify the pain due to injection at each angle, a questionary form was provided and filled by each patient right after the injection. In the form, patients need to give a pain score on a scale of 0–20 in a way that 0 stands for the lowest pain while 20 shows the highest pain (*$p < 0.05$ compared to 90°, **$p < 0.05$ compared to 90°, and ***$p < 0.05$ compared to 90°)
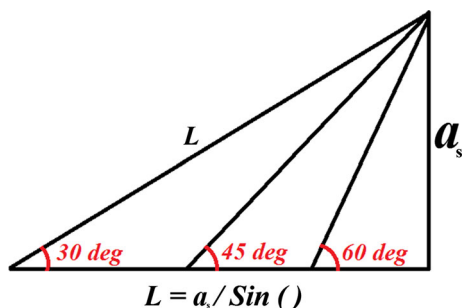
Fig. 8 The schematic configurations of **a** the normal and **b** oblique loadings

Fig. 10 The schematic of the distance that a needle would take up to deep injection into the tissue

$$\tau_{ave_{xy_{45°}}} = \frac{V}{A} = \frac{\sqrt{2}}{2}\sigma_{z_{90°}} \tag{7}$$

$$\tau_{\max_{xy_{45°}}} = \frac{3}{2}\frac{V}{A} = \frac{3}{2}\frac{\sqrt{2}}{2}\sigma_{z_{90°}} \tag{8}$$

where $\tau_{ave_{xy_{45°}}}$ and $\tau_{\max_{xy_{45°}}}$ are the average and maximum shear stresses in xy plane for state of 45°. Using Eqs. (2), (6), and (7), one easily finds:

$$\sigma_{z_{45°}} = \frac{1}{\sqrt{2}}\left\{3 + 2\left[\frac{\sqrt{2}}{2} \pm 3\sqrt{2}\left(\frac{h}{b^2}\right)z\Big|_{z=0}^{z=h}\right]^2\right\}^{1/2}\sigma_{z_{90°}} \tag{9}$$

where $\sigma'_{45°}$ displays the equivalent von Misses stress under angles of 45°. According to the above equations, it can be concluded that the equivalent von Misses stress for the case of 45° is $\frac{1}{\sqrt{2}}\left\{3 + 2\left[\frac{\sqrt{2}}{2} \pm 3\sqrt{2}\left(\frac{h}{b^2}\right)z\Big|_{z=0}^{z=h}\right]^2\right\}^{\frac{1}{2}}$ times of the equivalent von Misses stress for the state of 90° one which showed a good consistency was found between the analytical and numerical results. Overall, the results of this study suggested that the needle insertion into tissue set with angle of 90° can significantly reduce the maximum values of strain and stress distribution and, as a result, the sensitivity of nerve receptors and pain in response to the needling insertion decrease.

The score of the patients to the sense of pain due to injection were recorded and showed in Fig. 9. The numerical results were well confirmed by the experimental observations as the highest pain score was reported at the angle of 30° whereas the lowest one was reported at the angle of 90°. These results suggest that the injection at the angle of 90° must trigger the least pain and, as a result, least injury after the injection.

Another point that must be considered is that, the distance which the needle traveled from the skin into the blood vessel. Therefore, whatever the angle of penetration is reduced, the distance that the needle will take to reach into the vessel is larger. As a result, more tissue damage

would be occurred and, subsequently, there would be more pain (Fig. 10).

Although the current study found the most suitable angle of injection based on the amount of stresses and deformations, it is the authors' belief that the results are still promising and further research are required. The mechanical behavior of the tissues were considered to be elastic, while it is known that soft tissues may behave like a hyperelastic [25, 26], viscoelastic [27, 28], visco-hyperelastic [29, 30], or nonlinear anisotropic material [31, 32]. In addition, despite the authors tried to provide a boundary and loading condition as close as possible to that of the nature of the tissue, the behavior of the living tissue under load would be much more complicate than the simple static condition. Finally, as previously reported, study of needle–tissue interaction would provide a deep understanding about the behavior of different kind of materials under blunt loading, such as gels [33], skins, and muscles [34] and, consequently, provide a wide range of outlook for the medical robotics equipment to get improve in their performance [35].

4 Conclusion

The aim of this study was to numerically simulate the needle–tissue interaction in order to find the most effective angle of injection which provides less pain and injury to the tissues. To do this, a FE model of the needle and tissue were established and the needle at four different angles, such as 30°, 45°, 60°, and 90° were inserted to the tissue. The results revealed that alteration of the injection angle would have a significant effect on the amount of stresses and deformations in the tissue. During input needle catheterization, the maximum and minimum values of both stress and strain in the tissue set generated surrounding the needle tip and deep segments of tissue, respectively. The maximum strain of tissue set increases by increasing the angle of needle insertion. However, the angle of 90° exhibits the least amount of maximum strain in comparison with other angles i.e. 30°, 45°, and 60°. The highest value of maximum stress was determined at the angle of 45°, whereas the lowest on was observed at the angle of 90°. Finally, the results indicated that the angle of needle can play an important role in the femoral vein catheterization in terms of stress and strain distributions. The pain and injuries caused by the injection procedure will vary according to the angle of needle. For instance, insertion at the angle of 90° can significantly reduce the maximum values of strain and stress and, as a result, the sensitivity of nerve receptors and pain will decrease.

Compliance with ethical standards

Conflicts of interest None.

Ethical standard All the clinical processes that have been carried out in the current study were under the ethical rules of Tehran University of Medical Sciences based on the 2008 Declaration of Helsinki.

References

1. Alterovitz R, Goldberg K, Okamura A. Planning for steerable bevel-tip needle insertion through 2D soft tissue with obstacles. In: Proceedings of the 2005 IEEE international conference on robotics and automation, 2005, ICRA 2005. IEEE; 2005. p. 1640–5.

2. Romano C, Cecca E. A new method to reduce pin-prick pain of intra-muscular and subcutaneous injections. Minerva Anestesiol. 2005;71:609.

3. Alavi NM, Ataee M, Mohammadi M, Alireazei M, Shafiee M. The effectiveness of acupressure on intramuscular injection pain. Feyz J Kashan Univ Med Sci. 2008;11:14–8.

4. Zaybak A, Khorshid L. A study on the effect of the duration of subcutaneous heparin injection on bruising and pain. J Clin Nurs. 2008;17:378–85.

5. Miller SF, Sanz-Guerrero J, Dodde RE, Johnson DD, Bhawuk A, Gurm HS, et al. A pulsatile blood vessel system for a femoral arterial access clinical simulation model. Med Eng Phys. 2013;35:1518–24.

6. Finocchietti S, Nielsen M, Mørch CD, Arendt-Nielsen L, Graven-Nielsen T. Pressure-induced muscle pain and tissue biomechanics: a computational and experimental study. Eur J Pain. 2011;15:36–44.

7. Finocchietti S, Takahashi K, Okada K, Watanabe Y, Graven-Nielsen T, Mizumura K. Deformation and pressure propagation in deep tissue during mechanical painful pressure stimulation. Med Biol Eng Comput. 2013;51:113–22.

8. DiMaio SP, Salcudean SE. Needle insertion modeling and simulation. IEEE Trans Robot Autom. 2003;19:864–75.

9. Alja'afreh T. Investigating the needle dynamic response during insertion into soft tissue. Proc Inst Mech Eng Part H J Eng Med. 2010;224:531–40.

10. Keehan E, Gergely V. Catheter and specialty needle alloys. In: Medical device materials V: proceedings of the materials & processes for medical devices conference 2009, August 10–12, 2009. Minneapolis, MN, USA: ASM Int; 2010. p. 105.

11. Xu W, Frank T, Cuschieri A. Development of a shape memory alloy multiple-point injector for chemotherapy. Proc Inst Mech Eng Part H J Eng Med. 2005;219:213–7.

12. Podder T, Clark D, Sherman J, Fuller D, Messing E, Rubens D, et al. Effects of tip geometry of surgical needles: an assessment of force and deflection. In: IFMBE proceedings; 2005. p. 1727–983.

13. Mahvash M, Dupont PE. Mechanics of dynamic needle insertion into a biological material. IEEE Trans Biomed Eng. 2010;57:934–43.

14. Brett PN, Parker T, Harrison AJ, Thomas TA, Carr A. Simulation of resistance forces acting on surgical needles. Proc Inst Mech Eng Part H J Eng Med. 1997;211:335–47.

15. Reed KB, Okamura AM, Cowan NJ. Modeling and control of needles with torsional friction. IEEE Trans Biomed Eng. 2009;56:2905–16.

16. Okamura AM, Simone C, O'Leary MD. Force modeling for needle insertion into soft tissue. IEEE Trans Biomed Eng. 2004;51:1707–16.

17. Steele A, German M, Haas J, Lambert G, Meechan J. An in vitro investigation of the effect of bevel design on the penetration and withdrawal forces of dental needles. J Dent. 2013;41:164–9.

18. Boonma A, Narayan RJ, Lee Y-S. Analytical modeling and evaluation of microneedles apparatus with deformable soft tissues for biomedical applications. Comput Aided Des Appl. 2013;10:139–57.

19. Asadian A, Patel RV, Kermani MR. Dynamics of translational friction in needle–tissue interaction during needle insertion. Ann Biomed Eng. 2014;42:73–85.

20. Matthews A, Hutnik C, Hill K, Newson T, Chan T, Campbell G. Indentation and needle insertion properties of the human eye. Eye. 2014;28:880–7.

21. Labbaf S, Ghanbar H, Stride E, Edirisinghe M. Preparation of multilayered polymeric structures using a novel four-needle coaxial electrohydrodynamic device. Macromol Rapid Commun. 2014;35:618–23.

22. Aoyagi S, Izumi H, Fukuda M. Biodegradable polymer needle with various tip angles and consideration on insertion mechanism of mosquito's proboscis. Sens Actuators A Phys. 2008;143:20–8.

23. Yamaguchi S, Tsutsui K, Satake K, Morikawa S, Shirai Y, Tanaka HT. Dynamic analysis of a needle insertion for soft materials: arbitrary Lagrangian–Eulerian-based three-dimensional finite element analysis. Comput Biol Med. 2014;53:42–7.

24. Oldfield M, Dini D, Giordano G, Rodriguez y Baena F. Detailed finite element modelling of deep needle insertions into a soft tissue phantom using a cohesive approach. Comput Methods Biomech Biomed Eng. 2012;16:530–43.

25. Karimi A, Faturechi R, Navidbakhsh M, Hashemi SA. A non-linear hyperelastic behavior to identify the mechanical properties of rat skin under uniaxial loading. J Mech Med Biol. 2014;14:1450075–82.

26. Karimi A, Navidbakhsh M, Rezaee T, Hassani K. Measurement of the circumferential mechanical properties of the umbilical vein: experimental and numerical analyses. Comput Methods Biomech Biomed Eng. 2014;18:1418–26.

27. Karimi A, Haghighatnama M, Navidbakhsh M, Haghi AM. Measurement of the axial and circumferential mechanical properties of rat skin tissue at different anatomical locations. Biomed Eng. 2014;60:115–22.

28. Karimi A, Haghighatnama M, Shojaei A, Navidbakhsh M, Haghi AM, Sadati SJA. Measurement of the viscoelastic mechanical properties of the skin tissue under uniaxial loading. Proc Inst Mech Eng Part L J Mater Design Appl. 2015; 1464420715575169.

29. Karimi A, Navidbakhsh M. Measurement of the nonlinear mechanical properties of a poly(vinyl alcohol) sponge under longitudinal and circumferential loading. J Appl Polym Sci. 2014. doi:10.1002/app.40257.

30. Karimi A, Navidbakhsh M, Beigzadeh B. A visco-hyperelastic constitutive approach for modeling polyvinyl alcohol sponge. Tissue Cell. 2014;46:97–102.

31. Karimi A, Navidbakhsh M, Shojaei A. A combination of histological analyses and uniaxial tensile tests to determine the material coefficients of the healthy and atherosclerotic human coronary arteries. Tissue Cell. 2015;47:152–8.

32. Karimi A, Rahmati SM, Navidbakhsh M. Mechanical characterization of the rat and mice skin tissues using histostructural and uniaxial data. Bioengineered. 2015;6:153–60.

33. van Veen YR, Jahya A, Misra S. Macroscopic and microscopic observations of needle insertion into gels. Proc Inst Mech Eng Part H J Eng Med. 2012; 0954411912443207.

34. Jiang S, Li P, Yu Y, Liu J, Yang Z. Experimental study of needle–tissue interaction forces: effect of needle geometries, insertion methods and tissue characteristics. J Biomech. 2014;47:3344–53.

35. van Gerwen DJ, Dankelman J, van den Dobbelsteen JJ. Needle–tissue interaction forces—a survey of experimental data. Med Eng Phys. 2012;34:665–80.